HHS Public Access

Author manuscript

FASEB J. Author manuscript; available in PMC 2021 November 01.

Published in final edited form as:

FASEB J. 2020 November ; 34(11): 14850–14862. doi:10.1096/fj.201902308RR.

A 12-Lipoxygenase-Gpr31 signaling axis is required for pancreatic organogenesis in the zebrafish

Marimar Hernandez-Perez[1], **Abhishek Kulkarni**[2], **Niharika Samala**[3], **Cody Sorrell**[1], **Kimberly El**[1], **Isra Haider**[1], **Ansari Mukhtar Aleem**[4], **Theodore R Holman**[4], **Ganesha Rai**[5], **Sarah A Tersey**[1], **Raghavendra G Mirmira**[1,2,3,6], **Ryan M Anderson**[1,6]

[1]Department of Pediatrics, Center for Diabetes and Metabolic Diseases, Indiana University School of Medicine, Indianapolis, IN, USA

[2]Department of Biochemistry and Molecular Biology, Indiana University School of Medicine, Indianapolis, IN, USA

[3]Department of Medicine, Indiana University School of Medicine, Indianapolis, IN, USA

[4]Department of Chemistry and Biochemistry, University of California Santa Cruz, Santa Cruz, CA, USA

[5]National Center for Advancing Translational Sciences, National Institutes of Health, Rockville, MD, USA

[6]Department of Medicine, Kovler Diabetes Center, The University of Chicago, Chicago, IL, USA

Abstract

12-lipoxygenase (12-LOX) is a key enzyme in arachidonic acid metabolism, and alongside its major product, 12-HETE, plays a key role in promoting inflammatory signaling during diabetes pathogenesis. Although 12-LOX is a proposed therapeutic target to protect pancreatic islets in the setting of diabetes, little is known about the consequences of blocking its enzymatic activity during embryonic development. Here, we have leveraged the strengths of the zebrafish—genetic manipulation and pharmacologic inhibition—to interrogate the role of 12-LOX in pancreatic development. Lipidomics analysis during zebrafish development demonstrated that 12-LOX-generated metabolites of arachidonic acid increase sharply during organogenesis stages, and that this increase is blocked by morpholino-directed depletion of 12-LOX. Further, we found that either depletion or inhibition of 12-LOX impairs both exocrine pancreas growth and unexpectedly, the generation of insulin-producing β cells. We demonstrate that morpholino-mediated knockdown of GPR31, a purported G-protein coupled receptor for 12-HETE, largely phenocopies both the depletion and the inhibition of 12-LOX. Moreover, we show that loss of GPR31 impairs pancreatic bud fusion and pancreatic duct morphogenesis. Together, these data provide new insight into the requirement of 12-LOX in pancreatic organogenesis and islet formation, and additionally provide

Corresponding authors Raghavendra G. Mirmira, 900 E. 57th Street KCBD 8130, Chicago, IL 60637, USA; rmirmira@uchicago.edu; Ryan M. Anderson, 900 E. 57th Street KCBD 8130, Chicago, IL 60637, USA; ryananderson@uchicago.edu.

Authors Contribution

MHP, TRH, DJM, RGM and RMA designed research; MHP, NS, TRH, SAT, RGM, AK and RMA analyzed data; MHP, NS, CS, AK, AMA, GB, KE, IH, TRH, and RMA performed research; MHP, SAT, RGM, and RMA wrote the paper; All authors approved the final version of the manuscript.

evidence that its effects are mediated via a signaling axis that includes the 12-HETE receptor GPR31.

Keywords

Pancreas development; 12-lipoxygenase; zebrafish; Gpr31; β cells; exocrine tissue

Introduction

Diabetes mellitus stems from either an absolute or a relative deficiency of insulin—a peptide hormone secreted from the pancreatic β cells. Augmentation of pancreatic β cell mass, whether by reducing β cell loss or increasing β cell formation, would restore the glucoregulatory functions of the pancreas and is likely to be part of a stable cure for diabetes. The lipoxygenases (LOXs) are enzymes implicated in the pathogeneses of various inflammatory diseases, including diabetes (1). LOXs produce hydroperoxide fatty acids from arachidonic acid (AA), linoleic acid (LA) and other poly-unsaturated fatty acids in a stereo specific reaction (2). 12-hydroxyeicosatetraenoic acid (12-HETE) that is produced by the action of 12-LOX on AA (3), has been shown to promote cellular oxidative and endoplasmic reticulum stress in mouse and human pancreatic β cells (4-7), thereby exacerbating the effects of inflammation on β cell dysfunction and death in the setting of type 1 and type 2 diabetes.

The LOX enzymes are conserved across species, based both upon their genetic similarity as well as their tissue expression patterns and catalytic activities. In mice, *Alox15* is expressed in pancreatic islets and encodes a 12/15-LOX that generates 12-HETE:15-HETE in a 6:1 ratio (1). Genetic deletion of *Alox15* in mice protects against loss of β cell mass and prevents the development of both type 1 diabetes and obesity-related type 2 diabetes (7, 8). In humans, 12-LOX is encoded by the *ALOX12* gene, which is expressed in pancreatic islets and produces almost exclusively 12-HETE from AA (5). Moreover, 12-HETE levels are elevated in the serum of newly diagnosed individuals with type 1 diabetes (9). These data single out 12-LOX as a target for diabetes therapies. However, the varied expression and catalytic activity patterns among homologs of 12-LOX introduce complexity into the interpretation of the role of 12-LOX and its products on normal pancreatic cellular homeostasis.

Although conventional whole-body *Alox15* knockout mice appear to have normal pancreas development (8, 10), it is possible that a compensatory increase in the expression of the homologous gene *Alox12* could blunt the impact of loss of *Alox15* (11). Confoundingly, it is not feasible to explore their potential roles during development using a double knockout approach, owing to the close proximity of the *Alox12* and *Alox15* loci in mice. Thus, given the limitations imposed by differences between humans and mouse models, novel approaches and tools are needed to investigate 12-LOX roles in developmental biology. Here, we have used the zebrafish model system to study the roles of 12-LOX and its signaling, both because of its experimental attributes and because its capacity to reproduce aspects of human disease pathogenesis. Relevant to our study model is also the conserved

regulatory mechanism for pancreas organogenesis and differentiation between human and zebrafish (12). A homolog of 12-LOX is encoded by *alox12* in zebrafish, and this protein produces largely 12-HETE from AA, with 8-HETE as a minor product. Previous studies of 12-LOX during zebrafish development using antisense morpholino knockdown have described phenotypes that suggest that there is an early and pleiotropic developmental role for 12-LOX (13). However, the described phenotypes were particularly severe (lethal) and the effect of 12-LOX depletion on pancreas development was not considered.

We present here a phenotypic characterization of 12-LOX and its lipid products during pancreas organogenesis and β cell formation in zebrafish. For this purpose, we used several approaches to disrupt this pathway, including *alox12* antisense morpholinos and a small molecule inhibitor of 12-LOX. In addition, we investigated the role of the putative 12-HETE receptor Gpr31 using morpholino-directed depletion. We show similar deficiencies in pancreas morphogenesis result from the loss of either gene product, and thereby demonstrate a heretofore unappreciated role for 12-LOX in pancreas organogenesis likely acting through 12-HETE and its receptor Gpr31.

Materials and Methods

Zebrafish (Danio rerio) maintenance and strains.

All zebrafish transgenic lines were previously published, and raised in standard laboratory conditions at 28.5 °C. The following transgenic lines were used in the experiments: *Tg(ptf1a:GFP)*^{jh1} (14), *Tg(duct:GFP)*^{ia3} (15), *Tg(gcga:GFP)*^{ia1} (15), and *Tg(ins:dsRed)*^{m1018} (16). In addition, the novel transgenic line *Tg(ins:HAM)*^{iu1} was generated in order to co-label β cells with Hsa.HIST1H2BJ-mCherry (H2B-RFP) in their nuclei and with EGFP-CAAX upon their plasma membrane. This was accomplished by first constructing an in-frame fusion of Hsa.HIST1H2BJ-RFP (17) , P2A (18) , and GFP-CAAX using PCR. This cassette was subcloned into a meganuclease transgenesis vector that contained the zebrafish insulin promoter, and the resulting transgene construct was injected into zygotes as previously described (19). All animal procedures were conducted in accordance with NIH and OLAW guidelines and were approved by the Indiana University Institutional Animal Care and Use Committee.

LOX Expression and purification.

The zebrafish 12-LOX (zf12-LOX) expression plasmid was made by first amplifying the full length zebrafish coding sequence from a 72 hours post fertilization (hpf) cDNA library using the following primers: 5’-atgca ccacc atcac catca cgagt acaaa gtgac agtgg cca and 5’-atgga aaaca gcatc actat ttag, which appended a His tag to the N-terminus. The resulting amplicon was TA-cloned into pJet1.2 using a CloneJet kit (Thermo-Fisher) and sequenced. zf12-LOX was then subcloned into the pFB/6His-12HLO vector using standard restriction methods. The resulting pFastBac-zf12LOX plasmid was then utilized to express and purify zf12-LOX as was described previously (20). Briefly, zf12-LOX enzyme was expressed as a fusion protein, with a 6XHis tag on the N-terminus and was purified by an affinity column of nickel-iminodiacetic acid agarose using a Biorad FPLC. The purity of the protein was

greater than 90% as determined by SDS-PAGE and density analysis of the Bradford and silver stained gels.

UV-Vis-based IC_{50} assay.

IC50 values of ML127 against purified zf12-LOX were determined in the same way as the steady state kinetic assay described previously (21). The reactions were carried out in 25 mM HEPES buffer (pH 8.00), 0.01% Triton X-100 and 10 μM arachidonic acid. IC_{50} values was obtained by determining the enzymatic rate at six inhibitor concentrations and plotting them against inhibitor concentration, followed by a hyperbolic saturation curve fit. The data used for the saturation curve fits was performed in triplicate.

Pharmacological treatments.

Zebrafish embryos were collected and grown under standard conditions in egg water supplemented with (4 mM) 1-phenyl 2-thiourea (PTU). Pharmacological inhibitor of 12-Lipoxygenase (ML127 or DMSO vehicle), was then added to the egg water at 12 hpf and refreshed every 12 hours until embryos reached 72 hpf. The optimal concentration of ML127 (5 μM) was determined by dose curve, using *Tg(ptf1a:gfp)*^{ih1} embryos to visualize phenotypic readout. These embryos were observed for alterations in pancreas development without any gross alterations in overall morphology or viability.

Microinjection and morpholino design.

Morpholinos (MO) were purchased from Gene Tools, LLC, and were designed against sequences for *alox12* (ZDB-GENE-030131-1452) and *gpr31* (ZDB-GENE-070705-34) that were curated on zfin.org: *alox12 MO1* (5'-ccact gtcac tttgt actcc atctt, targeting the translational start (13)); *alox12 MO2* (5′-tcaat caatg taact gacct gtgcc, targeting the splice site at the junction of exon 4 and intron 4); *gpr31 MO1* (5'-gtgca gattc ccagt ccgag atgac targeting the translational start). To visualize and normalize the morpholino injections, Dextran-conjugated Alexa fluor (ThermoFisher #D34679) and 5% Phenol Red were co-injected into zygotes along with each morpholino. Efficacy of splicing disruption/knockdown of alox12 by *alox12 MO2* was evaluated by RT-PCR/agarose gel analysis, with RNA and cDNA prepared as below. The primers 5′-gaaag gaaag agcga gagga and 5′-gggca gatca gcttc acttt amplify across the predicted deletion to generate a 412 bp amplicon in control embryos.

RNA isolation and RT-qPCR.

RNA was isolated with an RNeasy micro kit (Qiagen #74004) and was used to prepare cDNA using a commercial kit (Applied Biosystems # 4368814). For whole embryo analysis of mRNA expression levels, 60-80 embryos per sample were collected at stages 1–4 dpf and 1 μg of RNA was used for cDNA preparation. For the tissue-specific expression studies, tissues were manually dissected from approximately 50 zebrafish at stages 3, 4, and 7 dpf, and were prepared in duplicate. The following tissue types were isolated: pancreas (p), liver (l), endoderm (e) other than pancreas and liver, and lastly the remainder (r) of embryo after dissection of all preceding tissues were pooled. 2 μg of isolated RNA was used to prepare cDNA as above. We also isolated mRNA from whole embryos at stages 1, 2, 3, 4 and 7 dpf

using the same clutches of embryos that were used for the specific tissue isolations with 2-4 biological replicates. The following primer sequences were used to amplify target sequences: *alox12* (5'-gacag tgacg tgcaa gagga and 5'-ctgcc acaaa caacg gacag), *gpr31* (5'-actaa gctgc ggaaa gccat and 5'-aaact gcttg ctgga tccga), *ef1a* (5'-ctgga ggcca gctca aacat and 5'-atcaa gaaga gtagt accgc tagca ttac), *pdx1* (5'-acacg cacgc atgga aagga ca and 5'-gcggg cgcga gatgt atttg tt), *insa* (5'-accat ggcag tgtgg cttca and 5'-caaag tcagc cacct cagtt), *beta actin1* (5'-cgagc aggag atggg aacc and 5'-caacg gaaac gctca ttgc) and *neuroD* (5'-acgca gcgct gtgat atacc ga and 5'-tcgcg ttcaa ctggg cgttc at). qPCR was performed using the SensiFAST™ SYBR® Lo-ROX Kit (Bioline #BIO-94002) following manufacturer's recommendations; briefly a three-step cycling of 40 cycles was used with an annealing temperature of 60°C.

In situ hybridization and immunofluorescence.

Whole mount immunofluorescent staining and cell quantifications were performed as previously described (22). For immunofluorescence the following antibodies were used: guinea pig anti-insulin (Biomeda #Ab2-ins); mouse anti-glucagon (Sigma #G2654); rabbit anti-dsRed (Clontech #632496);. Alexa Fluor-conjugated antibodies were used for visualization (Life Technologies), and DAPI (Invitrogen #D1306) or TO-PRO3 (ThermoFisher #T3605) was used to label cell nuclei. Whole mount *in situ* hybridization was performed as described (23); approximately 1 kb *alox12* and *gpr31* antisense probes were transcribed from templates that were PCR amplified from a 72 hpf embryonic cDNA library. Primers sets included a T7 promoter on the antisense primer, and were as follows: *alox12*, 5'- gcatg catta atacg actca ctata gggag aatgg aaaac agcat cacta tttag and 5'-atgga gtaca aagtg acagt ggcca; *gpr31*, 5'- gcatg catta atacg actca ctata gggag acaat catct gcggt gtcat c and 5'-aaccg agcgc tgtac atttt. BM purple (Roche Life Sciences) was used for colorimetric development and Vector Red (Vector Laboratories) was used for fluorescent visualization at 555nm. For Z stack imaging and cell quantification, embryos were imaged using an LSM 700 confocal microscope (Zeiss). Whole embryo images were captured with a M205 FA epifluorescence microscope (Leica). Cell quantification and pancreas length measurements were performed using NIH Image J software (24, 25).

Analysis of eicosanoids panel.

30 to 50 zebrafish embryos from each embryonic stage were collected and immediately frozen to analyze lipid content. Samples volumes were normalized based on embryo content and were analyzed by the Washington University Metabolomics Core Facility (https://research.wustl.edu/core-facilities/metabolomics-facility/) using published methods (26). The eicosanoid panel was comprised of 5-HETE, 8-HETE, 12-HETE, 15-HETE, 12-HEPE, 15-HEPE, 13-HODE, 14-HDHA, and 17-HDHA.

Total free glucose measurement in whole embryo lysates.

A colorimetric glucose assay (BioVision #K686) was used on zebrafish embryo lysates following manufacturer recommendations. Specifically: 10 embryos per condition were collected in 500 μL of sample buffer and stored at −20°C. Collected samples were then thawed on ice, homogenized, and cleared by centrifugation. 50 μL of each resulting

supernatant were used for each reaction. 3-4 biological replicates were prepared for each condition.

Statistical analysis.

Prism 7 software (GraphPad) was used for statistical analysis. Unless otherwise noted, data are presented as mean ± SEM. Two-tailed Student's t-test was used for comparisons involving two conditions, and comparison of larger groups was analyzed by one-way ANOVA with a Turkey post hoc test. In all cases, significance was indicated on the graph as follows: $p \leq 0.05$ (*), $p \leq 0.01$ (**), $p \leq 0.001$ (***).

Results

12-LOX products levels increase during zebrafish organogenesis.

To determine if lipoxygenases and their eicosanoid products might play a role specifically in pancreas development, we conducted a comprehensive lipidomics analysis measuring the levels of 12-LOX, 15-LOX, 5-LOX, and cyclooxygenase (COX)-derived products. The final lipid derivative of a given LOX depends on the polyunsaturated fatty acid that serves as substrate, as shown in Fig.1A. In our analysis, we measured the levels of a panel of LOX and (COX) lipid products that were extracted from embryos at developmental stages ranging from 1 to 4 days post fertilization (dpf). We found that the 12-LOX products 12-HETE, 12-HEPE and 14-HDHA were substantially more abundant than other lipoxygenase products, with a two orders-of-magnitude difference for 12-HETE and 12-HEPE. Furthermore, two-way ANOVA test showed significant elevation in the 12-LOX products 12-HETE, 12-HEPE and 14-HDHA, but not 8-HETE at later developmental stages (2, 3 and 4 dpf) as compared to 1 dpf (Fig 1B), a period during which most early organogenesis is largely completed. In contrast, most of the 5-LOX and 15-LOX products were detected at much lower levels, and these remained largely unaltered during all stages, with the exception of 15-HEPE and 17-HDHA, which were mildly increased (Fig 1C,D). Additional 5-LOX products (5-HEPE, 4-HDHA) and the COX product (9-HODE) were undetectable. In accordance with previous reports showing that zebrafish 12-LOX generates 12-HETE:8-HETE in a 13.5:1 ratio (13), we also found a similar ratio of these 12-LOX products. Together, these data indicate that 12-LOX products are produced at developmental stages consistent with a role in organogenesis.

12-LOX has a critical role in pancreas development

To elucidate the spatiotemporal expression of *alox12* during organogenesis, we examined the expression of *alox12* mRNA at multiple developmental stages. First, we quantified levels of *alox12* mRNA expression using quantitative PCR of cDNA produced from whole embryo extracts sampled throughout early organogenesis stages. For reference, we measured expression of *elongation factor 1 a* (*elfa)* since it shows little variation across early developmental stages, and thus it is an excellent benchmark throughout early organogenesis stages (27, 28). Highest levels of *alox12* expression were measured at 1 dpf and 2 dpf and this was followed by a decreasing trend in expression at 3 dpf (Fig 2A). On the other hand, levels of the pancreatic marker *pdx1* significantly increased at 3 dpf with another substantial increase at 4 dpf concurrent with growth of the pancreatic buds. Due to the lack of zebrafish-

specific antibodies for 12-LOX we could not directly assess protein levels by immunostaining or immunoblotting. Thus, to determine the specific embryonic regions of *alox12* expression, we used whole mount fluorescent *in situ* hybridization (ISH) to reveal that *alox12* is clearly expressed in pancreas in addition to other specific tissues at 72 hours post fertilization (hpf) (Fig 2B). We also generated cDNA from specific dissected tissues at 3, 4 and 7 dpf in order to quantify mRNA expression levels: pancreas (p), liver (l), residual endoderm (e) without pancreas or liver, and lastly, all remnant tissues (r) remaining after the dissections (Supplemental Figure 1). The detection of *insulin* almost exclusively in dissected pancreas tissue and *pdx1* in pancreas and endoderm tissues, indicates the specificity of the dissections. The expression pattern of *alox12* mRNA observed in all tissue samples is consistent with the expression observed in our ISH assay. These data, as with the lipidomics analysis, indicate that *alox12* is expressed in a spatiotemporal manner consistent with a role in pancreas organogenesis.

Next, to assess the function of 12-LOX during organogenesis we used antisense morpholinos (MOs) to knockdown expression of *alox12* in developing zebrafish by blocking translation (*alox12* MO1). A previous MO knockdown study (13) dosed zebrafish zygotes with approximately 10 ng of *alox12* MO1, which resulted in severe and pleiotropic phenotypes. In contrast, we injected lower doses of MO1— ranging from 2 to 4 ng—in an approach to identify more specific phenotypes, and thus reveal developmental roles that require the highest levels of 12-LOX. These *alox12* MO1-injected larvae exhibited a significant decrease in pancreas size of approximately 34% at 3 dpf, which was more penetrant at 4 ng (Fig. 2C,D). We also confirmed this diminished pancreatic phenotype using a second distinct MO (*alox12* MO2) that instead disrupts *alox12* pre-mRNA splicing (Supplemental Figure 2). However, in all further analyses described below, we exclusively used *alox12* MO1.

Next, to measure both the specificity and the efficacy of the *alox12* MO1 knockdown, we performed a lipidomic analysis to quantify the endogenous levels of key lipid products of 12-LOX, 15-LOX, and 5-LOX in wildtype and *alox12* MO1-injected animals. For this, lipids were isolated from pools of zebrafish larvae that were zygotically-injected with either 2 or 4 ng of *alox12* MO1. The *alox12* MO1-injected embryonic zebrafish extracts showed a statistically significant decrease in all tested 12-LOX products (12-HETE, 12-HEPE, 8-HETE and 14-HDHA) when either of the *alox12* MO1 concentrations was injected (Fig. 2E). Further, the 15-LOX product 15-HEPE was diminished by either dose of MO1 while in contrast, the other 15-LOX products (15-HETE and 13-HODE) and the 5-LOX product (5-HETE) and did not show significant changes (Fig. 2F).

The zebrafish protein orthologue of 12-LOX has 45% amino acid identity with human 12-LOX and 44% identity with mouse 12/15-LOX. Importantly, the crucial amino acids that comprise the catalytic triad and that predict its 12-lipoxygenase activity are conserved among human, mouse and zebrafish 12-LOXs. These catalytic residues are critical for the production of 12(S)-HETE versus 12(R)-HETE (29). These conserved features suggest functional conservation. Further, they suggest that ML127, a highly selective small molecule competitive inhibitor of human 12-LOX (30) would be effective in blocking zebrafish Alox12 activity. Therefore, to provide further evidence that the observed hypoplastic pancreas phenotype in *alox12* MO-injected zebrafish was due to the loss of 12-LOX activity,

we used two complementary pharmacological approaches. First, we performed an *in vitro* enzymatic assay to compare the potency of ML127 on human and zebrafish 12-LOX enzyme preparations. IC50 data show that the inhibitor ML127 has an inhibitory effect on both human and zebrafish 12-LOX homologues (95% and 33% maximum inhibition, respectively; Table 1). It should be noted that the max inhibition is low at 33%, which is most likely due to allosteric inhibition of zf12-LOX. In contrast, the inhibitor ML351, which blocks the activity of human ALOX15 but not ALOX12, showed no effect on zebrafish 12-LOX. Next, we treated embryos *in vivo* with 5 μM ML127 continuously from 0.5 to 3 dpf. This inhibitor treatment dramatically reduced exocrine pancreas length (2-fold decrease when compared to control), phenocopying the *alox12* MO1 knockdown (Fig 2G,H). In contrast, treatment with increasing concentrations of ML351 (at 10, 20 or 40 μM) had a mild effect on pancreas size resulting in an approximately 10% decrease in length as compared to vehicle-treated controls (Supplemental Figure 3A-B).

To further validate our loss-of-function phenotypes, we measured the same panel of lipids isolated from 3 dpf embryos that were treated with 5 μM ML127 for 12 hours (Fig. 2I,J). These ML127-treated embryos showed a significant reduction for all 12-LOX products and for 15-HEPE, 13-HODE and 5-LOX, Embryos treated with 15 μM of the 15-LOX specific inhibitor ML351 showed a more moderate reduction in levels of 12-HETE, all other 12-LOX products, and for 15-HEPE, 13-HODE and 5-LOX (Supplemental Figure 3E,F). Despite a dosage three times higher than ML127, ML351 shows around 30.4% decrease in 12-HETE compared with 63.3% decrease found with ML127. Together these data demonstrate both efficacy and specificity of *alox12MO1* for its target.

To determine if 12-LOX has a role in the development of the pancreatic islet during organogenesis, in addition to its role in the exocrine cells, we next examined the two most prominent endocrine cell populations: beta cells and alpha cells. To do this, we quantified β cells in *alox12* MO1-injected 3 dpf larvae using the newly generated transgenic line *Tg(ins:H2B-RFP-p2a-EGFP-CAAX)*^{iu1} (a.k.a. *ins-HAM* for H2B-RFP-p2a-Membrane-boundGFP) zebrafish in which each insulin-expressing β cell is marked with both a red nucleus and a green plasma membrane. We found that knockdown of *alox12* resulted in a significant 14% decrease in the quantity of β cells from 30.8 to 26.5 cells per islet (Fig 3A-C). In contrast, the quantity of α cells, which were identified with anti-glucagon immunostaining, did not change in the *alox12* MO1 injected embryos (46 vs. 48 α cells in control vs. *alox12MO1*; Fig 3D-F). Treatment with ML127 also caused a statistically significant reduction in beta cell number (Fig. 3G-I) although no change was found with ML351 (Supplemental Figure 3C-D). To determine whether there was a change in beta cell function, we next measured the level of free glucose in whole embryo lysates at 2 and 3 dpf. We found no differences with *alox12* MO1 injection or treatment with either ML127 or ML351 (Supplemental Figure 4A-B). These results demonstrate that the β cells and α cells have differential requirements for *alox12* during development.

Knockdown of gpr31 alters exocrine pancreas growth and is necessary for β cell formation

Based on both biochemical and functional studies, GPR31 and its murine orthologue Gpr31b have been proposed as receptors for 12-HETE (31, 32). Phylogenetic analysis suggests that

zebrafish also possess one orthologous gene, *gpr31* (Fig. 4A). During zebrafish development *gpr31* mRNA expression increases from 1 to 2 dpf, followed by relatively decreased levels at 3 and 4 dpf, reflecting a similar overall expression pattern to *alox12* mRNA (compare Fig. 4B and Fig. 2A). We examined the expression of *gpr31* by fluorescent whole mount in situ hybridization and detected transcript in the pancreas and other tissues at 72 hpf (Fig. 4C). We also measured the tissue-specific mRNA expression levels in pancreas and other tissues by qPCR as done with *alox12* (Supplemental Figure 1). The distribution of *gpr31* mRNA observed in these tissues are consistent with our findings using *in situ* hybridization, showing expression in pancreas and other examined tissues. These results show that *gpr31* is expressed appropriately to respond to 12-HETE that may be produced by 12-LOX in the pancreas.

To determine if Gpr31 functions as a downstream effector of 12-LOX and 12-HETE in pancreas development, we again used an antisense MO knockdown approach to block *gpr31* translation during development. Injection of as little as 2 ng of *gpr31* MO showed a hypoplastic pancreas phenotype similar to the *alox12* MO-injected embryos, although the phenotype is much more pronounced in the *gpr31* MO-injected embryos (286.1 μm vs. 104.5 μm; Fig. 4D-F). We performed a lipidomics analysis of *gpr31* MO-injected zebrafish and as expected we found no changes in any of the lipids in our panel (Fig. 4G,H).

Lastly, we asked whether the defect in pancreas formation observed in the *gpr31*MO-treated zebrafish was restricted to the hypoplastic exocrine tissue, or whether it also extended to endocrine cell formation as in the *alox12* MO-injected embryos. Similar to the *alox12* MO, we found a decrease of 21.8% in the number of β cells in *ins:HAM* zebrafish that were injected with 2 ng *gpr31* MO (28.9 vs. 22.6 β cells per islet; Fig. 5A-C). The glucagon-positive α cells were also quantified, but we observed no differences between islets of control and MO embryos (Fig 5D-F). Notably, we also observed that islet morphology was usually altered in *gpr31* MO-injected embryos. Normally, pancreatic endocrine cells are clustered in a single islet with a core of beta cells surrounded by a mantle of alpha cells (Fig. 5A,D). In *gpr31*MO-injected embryos, clustering and beta-alpha organization were disrupted. Despite these changes, we found no significant change in free glucose levels in the *gpr31* MO-injected embryos (Supplemental Figure. 4A). The similarity in phenotype, and absence of change in LOX products is consistent with a role for Gpr31 in the same pathway, but downstream from Alox12, implicating 12-HETE as the relevant lipid product.

Discussion

The Lipoxygenases comprise a family of homologous enzymes that oxygenate membrane-derived lipids to form lipid products that can alter cellular redox states and function. 12-LOX has been studied as a therapeutic target for diverse diseases, and recent studies in the context of diabetes suggest that this enzyme promotes proinflammatory responses in pancreatic islets (11, 33, 34). The development of multiple specific inhibitors of 12-LOX as potential therapeutics for diabetes underscores a need to reveal all consequences of diminished enzyme activity in pancreatic tissues; both in normal and diseased states, and also during pancreatic development.

To date, little is known about the role of 12-LOX-generated lipids in organ development. Notably, the knockouts of the genes encoding 12-LOX (*Alox12*) and the closely related 12/15-LOX (*Alox15*) in mice result in no clear developmental or post-developmental organ abnormalities (4, 35, 36). However, it is not possible to precisely determine the roles of these enzymes in normal tissues in mice, since both enzymes in mice catalyze formation the same major product, 12-HETE, from arachidonic acid (37). Hence, the loss of one enzyme is likely to compensate for the other in some contexts (11). Whereas a knockout of the both genes in mice would address this issue, the proximity of the two genes on mouse chromosome 11 makes this a technically challenging task. Our study was designed to address the roles played by 12-LOX in pancreas development using a simpler and more tractable, yet physiologically similar, model. In zebrafish, pancreas development and composition closely resembles that of mammals (12), yet the characteristics of optical transparency, availability of fluorescently-labeled transgenic lines, facility of morpholino-based gene knockdown, and simplicity of small molecule treatments together make the zebrafish a developmental system with unparalleled versatility to interrogate the developmental effects of 12-LOX depletion. Our studies, using a combination of MO- and small molecule-based approaches combined with targeted lipidomic analysis, shows for the first time that the 12-LOX is required for normal pancreatic exocrine and endocrine development, and suggests that these roles are likely mediated by a signaling axis involving 12-HETE and GPR31.

Although the presence of 12-HETE has been previously demonstrated in zebrafish embryos (13, 38, 39), our lipidomics assay measuring a panel of lipoxygenase products revealed a surge in the production of specific 12-LOX products that are derived from AA, EPA, and DHA between 2 and 4 dpf. Furthermore, the surge in 12-LOX products coincides with increased mRNA levels of *alox12*. In contrast, levels of 15-LOX and 5-LOX products were much lower or undetectable during this period. Although these findings do not exclude roles for 15-LOX and 5-LOX products, the striking abundance of 12-LOX products are suggestive of an important role for 12-LOX during organogenesis stages of development. Since at the developmental stages studied, zebrafish embryos do not feed, but rather only utilize nutrients from their yolk, the source of all lipid substrates are not dietary. Furthermore, the high levels of EPA and DHA-derived products are not likely to be unique to zebrafish since these fatty acids, particularly DHA have been shown to be essential for nervous system development in several species including humans (40, 41).

A prior study assessed the role of 12-LOX in zebrafish development by use of MO-based depletion of *alox12* mRNA (13). That study reported a strikingly severe pleiotropic phenotype that included deranged brain, eyes, skin, and tail development as well as pericardial and yolk sac edema. However, no alterations in pancreatic development were specifically reported. In contrast, in our study we observed clear defects in pancreatic organogenesis, with shortened pancreatic length together with a reduced mass of exocrine and endocrine cells, and relative sparing of other organ systems and features. We attribute these phenotypic differences to the differing MO dosages, which were substantially lower in our study. We argue that by using a lower dose of morpholino to knockdown *alox12*, that we have uncovered a pancreas-specific role for 12-LOX. The low levels of *alox12* mRNA expression in the pancreas are consistent with our finding that these tissues are more

sensitive to knockdown than others where the gene is more highly expressed. The specific role of 12-LOX in pancreas is further supported by two additional observations: First, morpholino-mediated depletion of *alox12* resulted in the predicted reductions in 12-LOX-generated lipids, but not in most lipids generated by 15-LOX or 5-LOX (with the exception of 15-HEPE). Second, small molecule-based inhibition of 12-LOX using ML127 also resulted in similar pattern of reduction of 12-LOX products a nearly identical pancreatic phenotype. While we cannot exclude the possibility that 15-HEPE is also a mediator of pancreas development, our similar results seen with GPR31 knockdown, which has not been shown to bind 15-HEPE (31), argue that 12-HETE is the major player.

It is important to note that we observed an approximately 10% more potent effect on pancreas length with ML127 treatment as compared to MO1, we attribute this to the different nuances of the drug and MO approaches. Since the MO molecule is injected at the zygote stage, its efficacy may be waning in the embryo by 3 dpf as it is diluted by each cell division. This stands in contrast to the drug treatment approach in which ML127 was continually replaced every 12 hours . Furthermore, as zebrafish have great regenerative and regulative capacities, any declines in MO concentration could provide opportunity for embryonic tissue to regenerate. Since the exocrine pancreas outgrowth occurs between 2.5 and 3.5 dpf , this phenotype cannot be quantified at earlier stages when morpholinos are likely to be more effective. In addition, since the potency of the inhibitors ML127 and ML351 was not tested against zebrafish Alox15 or Alox5, it is possible that they are also mildly affecting these or other homologues. Despite the fact that ML351 was used at a concentration three times greater than the concentration of ML127, the small reductions in pancreas size and 12- and 15-LOX products cause by ML351 treatment, might not be enough to have much biological impact on pancreas development; this idea is supported by the lack of reduced β cell number with ML351 treatment. The specificity showed by the *alox12* MO1 approach, which affects only 12-LOX products, and gpr31, with no effect on any LOX product, and the mild effect of ML351 suggest that the pancreas developmental phenotype observed is mainly due to the decreased in 12-LOX products rather than 15- or 5-LOX. Even though no differences were found in free glucose assays of the MO and drug treated embryos, disturbances in glucose regulation might be observed if the animal were to experience metabolic stress as has been shown for other mouse models of alox12/15 KO . Also, the decrease in MO concentration over time might also allow the remaining beta cells to compensate for they reduced number. We therefore conclude that 12-LOX is required for normal exocrine and endocrine pancreas development in zebrafish.

Among the lipids examined in this study, 12-HETE (derived from AA) and 12-HEPE (derived from EPA) were detected at the highest levels during the period of pancreatic organogenesis. Recently, a receptor for 12-HETE, GPR31, was identified (31). This GPCR exhibited high-affinity characteristics for 12-HETE (K_d ~ 4.8 nM) with specificity for the biologically-relevant *S*-enantiomer, highly selective for 12- vs 5- and 15- HETE, but GPR31 has not been reported to have affinity for 12-HEPE (31). Since 12-HEPE levels are comparable with 12-HETE levels in all stages we cannot discard the possibility that the observed effects are, at least in part, mediated by 12-HEPE. Nevertheless we can say the effect of GPR31 appears to be mostly through 12-LOX products. Furthermore, in studies *in vivo* using a hepatic ischemia-reperfusion injury model, it was demonstrated that the

injurious effects of 12-LOX were referable to the signaling induced upon binding of 12-HETE to GPR31 (32). A similar link between Gpr31 and 12-HETE was observed in prostate cancer (42). Our findings here, that knockdown of the *gpr31* homologue in zebrafish phenocopies the loss of 12-LOX activity, provide further support for a signaling axis comprised of 12-LOX, 12-HETE, and GPR31 during pancreatic organogenesis. The downstream mechanisms by which GPR31 exerts its effect on cellular growth and developmental properties is largely unknown. However, it has been shown that GPR31 regulates the association of KRAS with the plasma membrane, and that this is essential for the proliferation, survival, and macropinocytosis activities of KRAS-dependent cancer cells (43). Nonetheless, is not known if this pathway is a relevant component in the 12-LOX/12-HETE/GPR31signaling axis that is essential for pancreas organogenesis.

Taken together, our studies provide evidence for a specific role for 12-LOX in pancreatic organogenesis, and further links its actions to 12-HETE and its receptor GPR31. Our study highlights the need for further study of the role of specific LOX products in organ development, and specifically the role of GPR31 and its signaling pathway in this process. While the zebrafish represents a powerful model system that is both tractable and expedient, our studies have uncovered a novel role for 12-HETE generation and signaling in pancreas development whose translation to mammalian organ development needs to be tested.

Supplementary Material

Refer to Web version on PubMed Central for supplementary material.

Acknowledgements

The authors would like to acknowledge the technical assistance of Mr. Morgan Robertson and Naomi Riley. We also wish to thank the Washington University Lipidomics Core facility for measurement of eicosanoids. MHP was supported by training grant T32 DK064466 from the National Institutes of Health and JDRF Postdoctoral Award 3-PDF-2019-750-A-N. This work was supported by grant R01 DK105588 (to RGM) from the National Institutes of Health. This study utilized core services provided by the by NIH grant P30 DK097512 to Indiana University School of Medicine.

Nonstandard Abbreviations

AA	arachidonic acid
EPA	eicosapentaenoic acid
DHA	docosahexaenoic acid
dpf	days post fertilization
Gpr31	G-protein-coupled receptor 31
HETE	hydroxyeicosatetraenoic acid
LOX	lipoxygenase
MO	morpholino

References

1. Dobrian AD, Huyck RW, Glenn L, Gottipati V, Haynes BA, Hansson GI, Marley A, McPheat WL, and Nadler JL (2018) Activation of the 12/15 lipoxygenase pathway accompanies metabolic decline in db/db pre-diabetic mice. Prostaglandins Other Lipid Mediat. 136, 23–32 [PubMed: 29605541]
2. Brash AR, Jisaka M, Boeglin WE, Chang MS, Keeney DS, Nanney LB, Kasper S, Matusik RJ, Olson SJ, and Shappell SB (1999) Investigation of a second 15S-lipoxygenase in humans and its expression in epithelial tissues. Adv. Exp. Med. Biol 469, 83–89 [PubMed: 10667314]
3. Coffa G and Brash AR (2004) A single active site residue directs oxygenation stereospecificity in lipoxygenases: stereocontrol is linked to the position of oxygenation. Proc. Natl. Acad. Sci. U. S. A 101, 15579–15584 [PubMed: 15496467]
4. Cole BK, Morris MA, Grzesik WJ, Leone KA, and Nadler JL (2012) Adipose tissue-specific deletion of 12/15-lipoxygenase protects mice from the consequences of a high-fat diet. Mediators Inflamm. 2012, 851798 [PubMed: 23326022]
5. Grzesik WJ, Nadler JL, Machida Y, Nadler JL, Imai Y, and Morris MA (2015) Expression pattern of 12-lipoxygenase in human islets with type 1 diabetes and type 2 diabetes. J. Clin. Endocrinol. Metab 100, E387–395 [PubMed: 25532042]
6. Taylor-Fishwick DA, Weaver J, Glenn L, Kuhn N, Rai G, Jadhav A, Simeonov A, Dudda A, Schmoll D, Holman TR, Maloney DJ, and Nadler JL (2015) Selective inhibition of 12-lipoxygenase protects islets and beta cells from inflammatory cytokine-mediated beta cell dysfunction. Diabetologia 58, 549–557 [PubMed: 25417214]
7. Tersey SA, Maier B, Nishiki Y, Maganti AV, Nadler JL, and Mirmira RG (2014) 12-lipoxygenase promotes obesity-induced oxidative stress in pancreatic islets. Mol. Cell. Biol 34, 3735–3745 [PubMed: 25071151]
8. McDuffie M, Maybee NA, Keller SR, Stevens BK, Garmey JC, Morris MA, Kropf E, Rival C, Ma K, Carter JD, Tersey SA, Nunemaker CS, and Nadler JL (2008) Nonobese Diabetic (NOD) Mice Congenic for a Targeted Deletion of 12/15-Lipoxygenase Are Protected From Autoimmune Diabetes. Diabetes 57, 199–208 [PubMed: 17940120]
9. Hennessy E, Rakovac Tisdall A, Murphy N, Carroll A, O'Gorman D, Breen L, Clarke C, Clynes M, Dowling P, and Sreenan S (2016) Elevated 12-hydroxyeicosatetraenoic acid (12-HETE) levels in serum of individuals with newly diagnosed Type 1 diabetes. Diabet. Med. n/a-n/a
10. Bleich D, Chen S, Zipser B, Sun D, Funk CD, and Nadler JL (1999) Resistance to type 1 diabetes induction in 12-lipoxygenase knockout mice. J. Clin. Invest 103, 1431–1436 [PubMed: 10330425]
11. Conteh AM, Reissaus CA, Hernandez-Perez M, Nakshatri S, Anderson RM, Mirmira RG, Tersey SA, and Linnemann AK (2019) Platelet-type 12-lipoxygenase deletion provokes a compensatory 12/15-lipoxygenase increase that exacerbates oxidative stress in islet β-cells. J. Biol. Chem
12. Prince VE, Anderson RM, and Dalgin G (2017) Zebrafish Pancreas Development and Regeneration: Fishing for Diabetes Therapies. Curr. Top. Dev. Biol 124, 235–276 [PubMed: 28335861]
13. Haas U, Raschperger E, Hamberg M, Samuelsson B, Tryggvason K, and Haeggström JZ (2011) Targeted knock-down of a structurally atypical zebrafish 12S-lipoxygenase leads to severe impairment of embryonic development. Proc. Natl. Acad. Sci. U. S. A 108, 20479–20484 [PubMed: 22143766]
14. Godinho L, Mumm JS, Williams PR, Schroeter EH, Koerber A, Park SW, Leach SD, and Wong ROL (2005) Targeting of amacrine cell neurites to appropriate synaptic laminae in the developing zebrafish retina. Development 132, 5069–5079 [PubMed: 16258076]
15. Pauls S, Zecchin E, Tiso N, Bortolussi M, and Argenton F (2007) Function and regulation of zebrafish nkx2.2a during development of pancreatic islet and ducts. Dev. Biol 304, 875–890 [PubMed: 17335795]
16. Shin CH, Chung W-S, Hong S-K, Ober EA, Verkade H, Field HA, Huisken J, and Y R Stainier D (2008) Multiple roles for Med12 in vertebrate endoderm development. Dev. Biol 317, 467–479 [PubMed: 18394596]
17. Hesselson D, Anderson RM, and Stainier DYR (2011) Suppression of Ptf1a activity induces acinar-to-endocrine conversion. Curr. Biol. CB 21, 712–717 [PubMed: 21497092]

18. Kim JH, Lee S-R, Li L-H, Park H-J, Park J-H, Lee KY, Kim M-K, Shin BA, and Choi S-Y (2011) High cleavage efficiency of a 2A peptide derived from porcine teschovirus-1 in human cell lines, zebrafish and mice. PLoS ONE 6, e18556 [PubMed: 21602908]

19. Hesselson D, Anderson RM, Beinat M, and Stainier DYR (2009) Distinct populations of quiescent and proliferative pancreatic beta-cells identified by HOTcre mediated labeling. Proc. Natl. Acad. Sci. U. S. A 106, 14896–14901 [PubMed: 19706417]

20. Amagata T, Whitman S, Johnson TA, Stessman CC, Loo CP, Lobkovsky E, Clardy J, Crews P, and Holman TR (2003) Exploring sponge-derived terpenoids for their potency and selectivity against 12-human, 15-human, and 15-soybean lipoxygenases. J. Nat. Prod 66, 230–235 [PubMed: 12608855]

21. Aleem AM, Tsai W-C, Tena J, Alvarez G, Deschamps J, Kalyanaraman C, Jacobson MP, and Holman T (2019) Probing the Electrostatic and Steric Requirements for Substrate Binding in Human Platelet-Type 12-Lipoxygenase. Biochemistry 58, 848–857 [PubMed: 30565457]

22. Ye L, Robertson MA, Hesselson D, Stainier DYR, and Anderson RM (2015) glucagon is essential for alpha cell transdifferentiation and beta cell neogenesis. Dev. Camb. Engl 142, 1407–1417

23. Thisse C and Thisse B (2008) High-resolution in situ hybridization to whole-mount zebrafish embryos. Nat. Protoc 3, 59–69 [PubMed: 18193022]

24. Mastracci TL, Robertson MA, Mirmira RG, and Anderson RM (2015) Polyamine biosynthesis is critical for growth and differentiation of the pancreas. Sci. Rep 5, 13269 [PubMed: 26299433]

25. Ye L, Robertson MA, Mastracci TL, and Anderson RM (2016) An insulin signaling feedback loop regulates pancreas progenitor cell differentiation during islet development and regeneration. Dev. Biol 409, 354–369 [PubMed: 26658317]

26. Masoodi M, Mir AA, Petasis NA, Serhan CN, and Nicolaou A (2008) Simultaneous lipidomic analysis of three families of bioactive lipid mediators leukotrienes, resolvins, protectins and related hydroxy-fatty acids by liquid chromatography/electrospray ionisation tandem mass spectrometry. Rapid Commun. Mass Spectrom. RCM 22, 75–83 [PubMed: 18059001]

27. McCurley AT and Callard GV (2008) Characterization of housekeeping genes in zebrafish: male-female differences and effects of tissue type, developmental stage and chemical treatment. BMC Mol. Biol 9, 102 [PubMed: 19014500]

28. Tang R, Dodd A, Lai D, McNabb WC, and Love DR (2007) Validation of Zebrafish (Danio rerio) Reference Genes for Quantitative Real-time RT-PCR Normalization. Acta Biochim. Biophys. Sin 39, 384–390 [PubMed: 17492136]

29. Jansen C, Hofheinz K, Vogel R, Roffeis J, Anton M, Reddanna P, Kuhn H, and Walther M (2011) Stereocontrol of Arachidonic Acid Oxygenation by Vertebrate Lipoxygenases NEWLY CLONED ZEBRAFISH LIPOXYGENASE 1 DOES NOT FOLLOW THE ALA-VERSUS-GLY CONCEPT. J. Biol. Chem 286, 37804–37812 [PubMed: 21880725]

30. Kenyon V, Rai G, Jadhav A, Schultz L, Armstrong M, Jameson JB, Perry S, Joshi N, Bougie JM, Leister W, Taylor-Fishwick DA, Nadler JL, Holinstat M, Simeonov A, Maloney DJ, and Holman TR (2011) Discovery of Potent and Selective Inhibitors of Human Platelet-Type 12- Lipoxygenase. J. Med. Chem 54, 5485–5497 [PubMed: 21739938]

31. Guo Y, Zhang W, Giroux C, Cai Y, Ekambaram P, Dilly A, Hsu A, Zhou S, Maddipati KR, Liu J, Joshi S, Tucker SC, Lee M-J, and Honn KV (2011) Identification of the Orphan G Protein-coupled Receptor GPR31 as a Receptor for 12-(S)-Hydroxyeicosatetraenoic Acid. J. Biol. Chem 286, 33832–33840 [PubMed: 21712392]

32. Zhang X-J, Cheng X, Yan Z-Z, Fang J, Wang X, Wang W, Liu Z-Y, Shen L-J, Zhang P, Wang P-X, Liao R, Ji Y-X, Wang J-Y, Tian S, Zhu X-Y, Zhang Y, Tian R-F, Wang L, Ma X-L, Huang Z, She Z-G, and Li H (2018) An ALOX12-12-HETE-GPR31 signaling axis is a key mediator of hepatic ischemia-reperfusion injury. Nat. Med 24, 73–83 [PubMed: 29227475]

33. Hernandez-Perez M, Chopra G, Fine J, Conteh AM, Anderson RM, Linnemann AK, Benjamin C, Nelson JB, Benninger KS, Nadler JL, Maloney DJ, Tersey SA, and Mirmira RG (2017) Inhibition of 12/15-Lipoxygenase Protects Against β-Cell Oxidative Stress and Glycemic Deterioration in Mouse Models of Type 1 Diabetes. Diabetes 66, 2875–2887 [PubMed: 28842399]

34. Luci D, Jameson JB, Yasgar A, Diaz G, Joshi N, Kantz A, Markham K, Perry S, Kuhn N, Yeung J, Schultz L, Holinstat M, Nadler J, Taylor-Fishwick DA, Jadhav A, Simeonov A, Holman TR, and

Maloney DJ (2010) Discovery of ML355, a Potent and Selective Inhibitor of Human 12-Lipoxygenase In Probe Reports from the NIH Molecular Libraries Program National Center for Biotechnology Information (US), Bethesda (MD)

35. Johnson EN, Brass LF, and Funk CD (1998) Increased platelet sensitivity to ADP in mice lacking platelet-type 12-lipoxygenase. Proc. Natl. Acad. Sci. U. S. A 95, 3100–3105 [PubMed: 9501222]
36. Sun D and Funk CD (1996) Disruption of 12/15-Lipoxygenase Expression in Peritoneal Macrophages ENHANCED UTILIZATION OF THE 5-LIPOXYGENASE PATHWAY AND DIMINISHED OXIDATION OF LOW DENSITY LIPOPROTEIN. J. Biol. Chem 271, 24055–24062 [PubMed: 8798642]
37. Kuhn H, Banthiya S, and van Leyen K (2015) Mammalian lipoxygenases and their biological relevance. Biochim. Biophys. Acta 1851, 308–330 [PubMed: 25316652]
38. Lebold KM, Kirkwood JS, Taylor AW, Choi J, Barton CL, Miller GW, La Du J, Jump DB, Stevens JF, Tanguay RL, and Traber MG (2013) Novel liquid chromatography-mass spectrometry method shows that vitamin E deficiency depletes arachidonic and docosahexaenoic acids in zebrafish (Danio rerio) embryos. Redox Biol. 2, 105–113 [PubMed: 24416717]
39. Zarini S, Hankin JA, Murphy RC, and Gijón MA (2014) Lysophospholipid acyltransferases and eicosanoid biosynthesis in zebrafish myeloid cells. Prostaglandins Other Lipid Mediat. 113–115, 52–61
40. Innis SM (2008) Dietary omega 3 fatty acids and the developing brain. Brain Res. 1237, 35–43 [PubMed: 18789910]
41. Igarashi M, Santos RA, and Cohen-Cory S (2015) Impact of maternal n-3 polyunsaturated fatty acid deficiency on dendritic arbor morphology and connectivity of developing Xenopus laevis central neurons in vivo. J. Neurosci. Off. J. Soc. Neurosci 35, 6079–6092
42. Honn KV, Guo Y, Cai Y, Lee M-J, Dyson G, Zhang W, and Tucker SC (2016) 12-HETER1/GPR31, a high-affinity 12(S)-hydroxyeicosatetraenoic acid receptor, is significantly up-regulated in prostate cancer and plays a critical role in prostate cancer progression. FASEB J. Off. Publ. Fed. Am. Soc. Exp. Biol 30, 2360–2369
43. Fehrenbacher N, Tojal da Silva I, Ramirez C, Zhou Y, Cho K-J, Kuchay S, Shi J, Thomas S, Pagano M, Hancock JF, Bar-Sagi D, and Philips MR (2017) The G protein-coupled receptor GPR31 promotes membrane association of KRAS. J. Cell Biol 216, 2329–2338 [PubMed: 28619714]

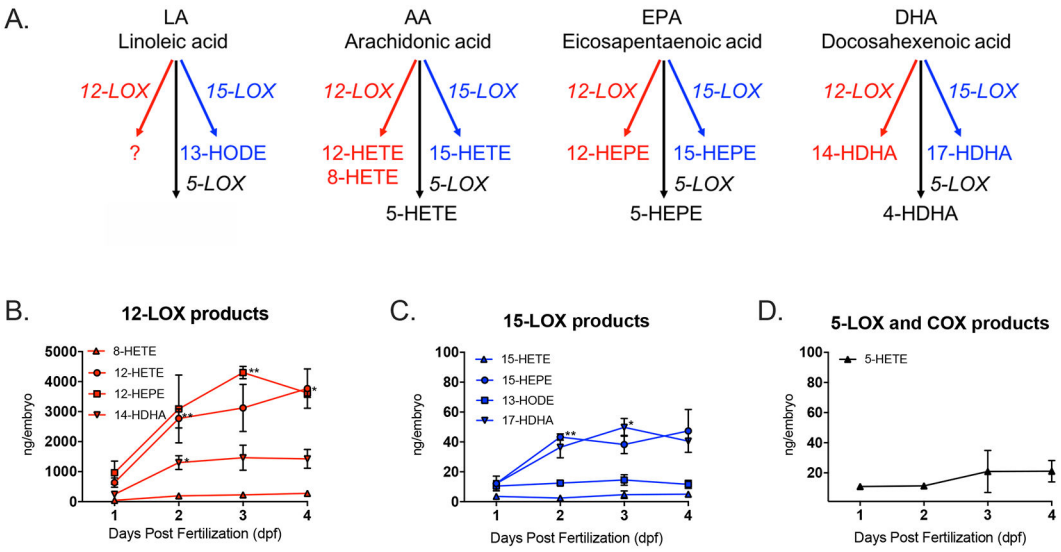

Figure 1. Lipidomic analysis of lipoxygenase products during early zebrafish development.

(A) Schematic depiction of the eicosanoid products of 12-, 5- and 15-Lipoxygenase that are derived from lipid substrates Linoleic Acid (LA), Arachidonic Acid (AA), Docosahexenoic Acid (DHA), and Eicosapentainoic Acid (EPA). (B-D) Two-Way ANOVA was performed for all the lipid products and mRNA comparing amount on each stage (2, 3 and 4 dpf) to 1 dpf. Lipidomic analysis of 12-, 15-, and 5-LOX products in zebrafish embryos aged 1 to 4 days post fertilization (dpf); lipid levels at each age are expressed as nanograms detected normalized to number of embryos (ng/embryos) in each sample. (B) 12-LOX products 12-HETE (triangle) and 12-HEPE (diamond) showed the highest levels, and also the largest increases during development. (C) 15-LOX products 13-HODE, 15-HEPE, 15-HETE, and 17-HDHA showed low levels of expression. (D) 5-LOX products 5-HEPE, 4-HDHA, and 9-HODE were undetectable in embryos; 5-HETE was detected at a low level that remained constant during these stages.

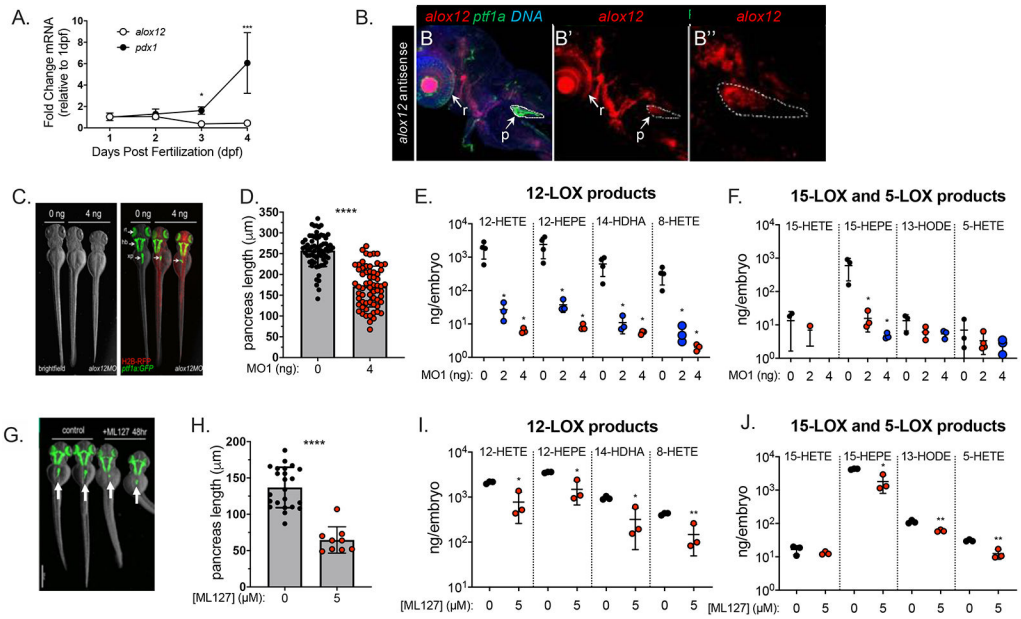

Figure 2. Expression of *alox12* mRNA in pancreatic development

(A) Quantitative PCR showing expression levels of *alox12* mRNA and *pdx1* mRNA throughout embryonic stages 1 dpf through 4 dpf. Levels are normalize to *elfa* mRNA and depicted as the relative expression level at 1 dpf. Two-way ANOVA was used to compare 2, 3, and 4 dpf levels with 1dpf. (B-B'') Merged (B), single channel (B'), and single channel inset (B'') confocal image of 3 dpf *Tg(ptf1a:GFP)*^{jh1} transgenic embryo with expression of *alox12* marked by fluorescent whole mount *in situ* hybridization (red). Green *ptf1a*-GFP signal is detected in the retina (r), pancreas (p), liver (L), heart (H), endoderm (E) and central nervous system. Red signal for *alox12* is detected throughout the green fluorescent pancreatic region. DNA is marked by TOPRO-3 (blue). (C) *Tg(ptf1a:GFP)*^{jh1} zebrafish embryos injected with 0 ng or 4 ng of *alox12* antisense morpholino (*alox12* MO1) as zygotes shown at 3 dpf. (C, right panel) Brightfield-only image shows no overt aberrant phenotypes in the knockdown embryos. (C, left panel) Merged image showing GFP expression (green) in the exocrine pancreas (xp), hindbrain (hb), and retina (rt) and the H2B-RFP marker of injection; zebrafish injected with 4 ng MO1 show shortened pancreas phenotype. (D) Quantification of GFP+ exocrine pancreas length shows a significant shortening by 33.6% ($p < 0.0001$). (E) 3 dpf *Tg(ptf1a:GFP)*^{jh1} zebrafish embryos treated with vehicle control or 5 μM of the ALOX12 inhibitor ML127 for 48 hr (from 12 h post fertilization to 3 dpf). ML127 treated embryos show slight developmental delay, but substantially truncated pancreas length (arrows), phenocopying the *alox12*-morpholino knockdown embryos. (F) Quantification of the GFP+ exocrine pancreas length shows a dramatic and highly significant shortening by 52.8% ($p<0.0001$). (G-I) Lipidomic analysis of products generated by 12-LOX (G), 15-LOX (H), and 5-LOX (I), in zebrafish injected with 2 ng or 4 ng of *alox12* morpholino and 0 ng controls.(*t*-test, p value <0.05 *). (G) All tested 12-LOX products, 12-HETE, 12-HEPE, 14-HDHA, and 8-HETE were essentially eliminated in animals injected with either dose of morpholino (showing one order of magnitude difference between control and injected). (H) The 15-LOX product, 15-HEPE, was expressed at lower levels but not statistically significant (*t*-test, $p = 0.0583$ for control vs

4 ng). 13-HODE remained unchanged (*t*-test, p = 0.116 for control vs 4ng). 15-HETE was undetectable in all 4ng samples and in. some control and 2 ng samples, between the detected samples no statistical difference was found (*t*-test, p = 0.1393). 17-HDHA was undetectable. (I) The 5-LOX product remained unchanged (*t*-test, p = 0.3379). (J-L) Lipidomic profile of LOX products from 3 dpf embryos treated with 5 uM ML127 for 12 hrs. T-test was used to compared treatment with control group. (J) Statistically significant reduction was observed for all 12-LOX products. (K) 15-LOX products, 15-HEP and 13-HODE, are significant reduced. 15-HETE does not changes and 17-HDHA was undetectable. (L) 5-LOX product, 5-HETE, is significantly reduced. 5-HEPE, 9-HODE and 4-HDHA were not detected.

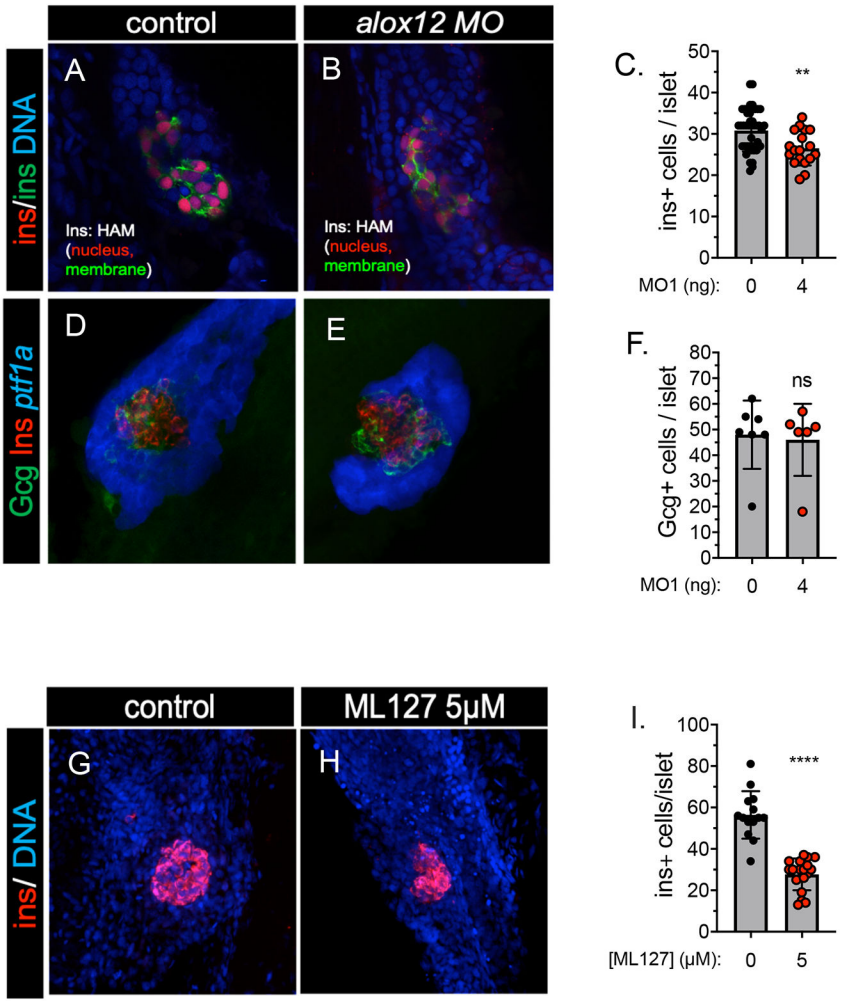

Figure 3. Islet composition of *alox12* morpholino knockdown embryos.

(A-C) Confocal image slices (A,B) and quantification (C) of the endocrine pancreas in *Tg(ins:HAM)*^{iu1} embryos injected with 0 ng (A) or 4 ng (B) of *alox12* morpholino. HAM- marks β cells with a red nucleus and green plasma membrane; DNA is stained with TOPRO-3 and is indicated in blue. (A) The head of the pancreas contains a compact principal islet comprised of an average of approximately 31 β cells. (B) The principal islet of *alox12* morpholino-injected embryos is slightly smaller, averaging approximately 26.5 β cells, and is dysmorphic. (C) Quantification of insulin-transgene marked β cells shows a significant decrease of the β cell mass in morpholino-injected animals (t-test, p=.002). (D-F) Confocal image projections (D,E) and quantification (F) of the endocrine pancreas in *Tg(ptf1a:GFP)*^{ih1} embryos injected with 0 ng (D) or 4 ng (E) of *alox12* morpholino. Insulin and glucagon were immuno-labeled, and are represented in red and green, respectively; GFP is represented in blue. (D) The principal islet has a core of β cells surrounded by a mantle of an average of approximately 48 glucagon-positive α cells. (E) The islet of *alox12* morpholino-injected embryos averaged approximately 46 β cells. (F) The number of α cells was not significantly changed (t-test, p = 0.7972). (G-I) Confocal images slices (G, H) of principal islet showing β cells on red (ins) and nucleous in blue (TOPRO) and quantification

(I) in embryos 3dpf embryos treated with 5 uM ML127 from 12 hpf to 3 dpf (t-test, $p < 0.0001$ ****) .

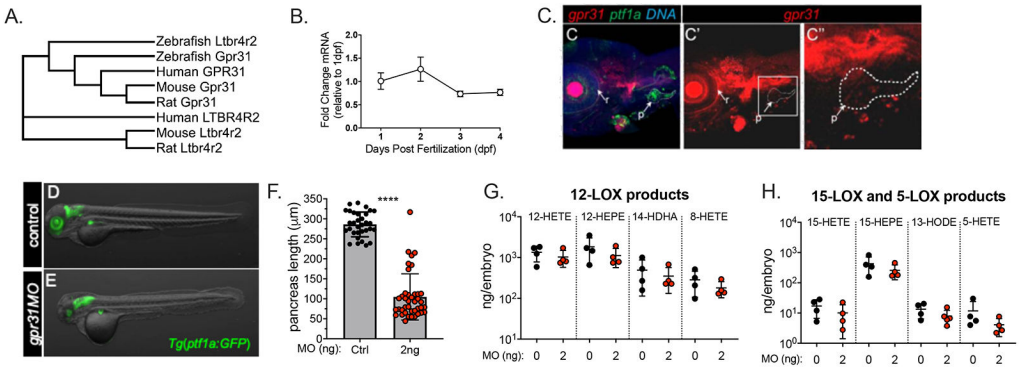

Figure 4. Pancreatic expression of the zebrafish orthologue of the 12-HETE receptor *gpr31*.

(A) Phylogenetic relationship among GPR31 orthologues in *Homo sapiens*, *Danio rerio* (fish), *Mus musculus* (mouse), and *Rattus norvegicus* (rat) and the closely related G protein coupled receptor LTB4R2 generated by Clustal Omega analysis of peptide sequences. Zebrafish Gpr31 clusters together with the mammalian homologues. (B) Quantitative PCR analysis showing expression levels of *gpr31* mRNA at embryonic stages from 1 dpf through 4 dpf. Levels are depicted as relative to the ubiquitously expressed gene *elfa* and were normalized to the relative expression level at 1 dpf. Global expression of *gpr31* peaks at 2 dpf. (C-C'') Merged (C), single channel (C'), and single channel inset (C'') confocal image of 3 dpf *Tg(ptf1a:GFP)*^{jh1} transgenic embryo with expression of *gpr31* marked by fluorescent whole mount *in situ* hybridization (red). Signal for *gpr31* is detected throughout the green fluorescent pancreatic region (p). DNA is marked by TOPRO-3 (blue). (D,E) *Tg(ptf1a:GFP)*^{jh1} zebrafish embryos injected with 0 ng (D) or 2 ng (E) of *gpr31* antisense morpholino as zygotes; shown at 3 dpf. (D) Control embryo shows GFP expression (green) in the exocrine pancreas (xp), hindbrain (hb), and retina (rt) (E) zebrafish injected with 2 ng *gpr31*MO show a severe shortened pancreas phenotype. (F) Quantification of GFP+ exocrine pancreas length shows an impressive and highly significant shortening of 63.6% ($p < 0.0001$). Lipidomic analysis of LOX products from 3 3dpf embryos injected with 2mg Gpr31 MO. (I) 12-LOX products from Gpr31 MO, 12-HETE, 12-HEPE, 14-HDHA and 8-HETE, no significant difference (t-test, p = > 0.05). (J) 15-LOX products from Gpr31 MO, 15-HETE, 15-HEPE and 13-HODE; no significant difference (t-test, p = > 0.05). 17-HDHA non detectable (K) 5-LOX products from Gpr31 MO, 5-HETE, no significant difference (t-test, p = > 0.05). 5-HEPE, 9-HODE and 4-HDHA non detectable.

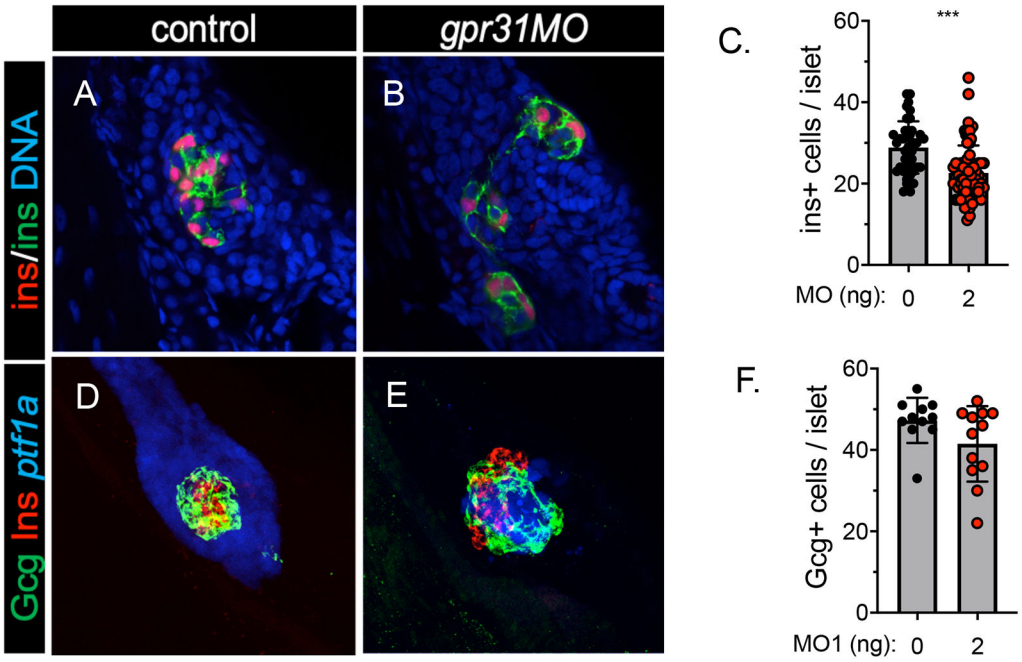

Figure 5. *gpr31* knockdown disrupts endocrine pancreas formation.

(A-C) Confocal image slices (A,B) and quantification (C) of the endocrine pancreas in *Tg(ins:HAM)*^{iu1} embryos injected with 0 ng (A) or 2 ng (B) of *gpr31* morpholino. β cells are marked with a red nucleus and green plasma membrane; DNA is stained with TOPRO-3 and is indicated in blue. (A) The control principal islet contained an average of approximately 29 β cells. (B) The principal islet of *gpr31* morpholino-injected embryos was smaller, and often fragmented, averaging approximately 22.6 β cells. (C) Quantification of β cells shows a significant decrease of the β cell mass by 22% in morpholino-injected animals (t-test, $p < 0.0001$). (D-F) Confocal image projections (D,E) and quantification (F) of the endocrine pancreas in *Tg(ptf1a:GFP)*^{jh1} embryos injected with 0 ng (D) or 2 ng (E) of *gpr31* morpholino. Insulin and glucagon were immuno-labeled in red and green, respectively; GFP is represented in blue. (D) The principal islet contained an average of approximately 47.2 glucagon-positive α cells, and (E) the islet of *alox12* morpholino-injected embryos averaged approximately 38.3 β cells. (F) The difference in the number of α cells approached, but did not reach, statistical significance (t-test, $p = 0.0673$).

Table 1.

Inhibitor activity in zebrafish and human 12-LOX enzyme.

Table shows IC_{50} and Max Inhibition determined for ML351 and ML127 in enzymatic assay using purified zebrafish and human 12-LOX.

Zebrafish Alox12	**IC_{50} (μM)**	**Max Inhibition**
ML127	0.34 +/− 0.3	33%
ML351	>100	
Human ALOX12	**IC_{50} (μM)**	**Max Inhibition**
ML127	1.0 +/− 0.2	95%
ML351	>50	